This is the author's version of an article that has been published in this conference. Changes were made to this version by the publisher prior to publication. The final version is available at http://dx.doi.org/10.1109/LAMC63321.2025.10880547

Optimizing the Full Mixed-Mode Performance of a Differential Microstrip Interconnect with a Right-Angle Bend by using Two Symmetrical Bumps

Enrique R. Villa-Loustaunau[#1], José E. Rayas-Sánchez[#2], Roberto Loera-Díaz[#$3], and Francisco Rangel-Patiño[#♣4]

[#]ITESO – The Jesuit University of Guadalajara, Tlaquepaque, Jalisco, 45604 Mexico

[$]Continental Automotive Group, Tlaquepaque, Jalisco, 45601 Mexico

[♣]Intel Corp. Zapopan, Jalisco, 45019 Mexico

[1]ervillal@iteso.mx, [2]erayas@iteso.mx, [3]roberto.loera@continental-corporation.com, [4]francisco.rangel@intel.com

***Abstract*—Differential interconnects are widely used for high-speed serial data transmission in modern high-performance computer platforms. Differential signaling handle noise better than single ended signaling. However, physical asymmetries and discontinuities in differential links can cause that a portion of the differential energy is converted into common mode (CM) energy, which is perceived as noise at the receiver. This mode conversion in differential interconnects leads to electromagnetic (EM) interference and EM susceptibility, limiting high data rates. In this paper, a microstrip differential interconnect with a severe discontinuity, a right-angle bend, is optimally compensated by using two rectangular length-match bumps. Our formulation allows the efficient optimization of the full set of mixed-mode (MM) S-parameters of the differential interconnect. It uses a smart combination of pattern search and Nelder-Mead to optimize the MM performance considering several starting points. The interconnect MM performance before and after optimization is shown, confirming a very significant performance improvement.**

***Keywords*—common mode, differential pair, discontinuity, high-speed interconnect, length match bump, mixed-mode S-parameters, mode conversion, Nelder-Mead, noise, optimization, pattern search, PCB, symmetry.**

I. Introduction

Modern high-performance computer platforms require transmitting high-speed data across multiple elements of the physical channel, such as the silicon die interconnections, the integrated circuit packages, component's pins, printed circuit board traces, vias, connectors, and cables, among others. These elements affect the transmitted signal in multiple manners. For instance, part of the energy is lost in the channel in the form of heat, or can be absorbed by the dielectrics, or reflected due to impedance discontinuities, or degraded due to electromagnetic (EM) interference, or radiated by undesired EM emissions, etc.

Many of the signal integrity issues observed in high-speed interconnects can be mitigated by using differential signaling. In most cases, differential signaling is more immune to noise and less severely impacted by discontinuities (*e.g.*, vias, bends, etc.) than single-ended (SE) signaling [1]-[3]. In practice, some discontinuities cannot be avoided, and many of them produce asymmetries in the differential structures [4]. These imbalances produce mode conversion: undesired common mode (CM) signals appear at the receiver as noise [3], [4], limiting the maximum communication data rates. These asymmetries must be compensated to improve signal integrity.

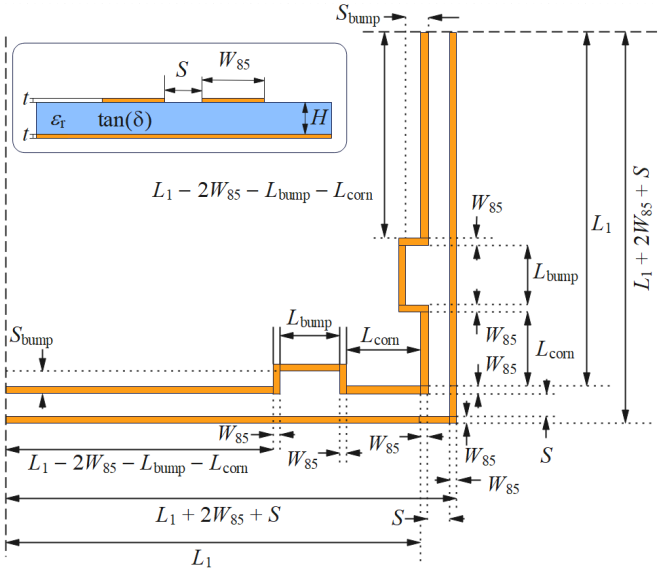

Fig. 1. Top view of a differential interconnect geometry with a 90° turn and two symmetric length match bumps. The cross-section view of the differential pair structure (ignoring the bumps) is included.

For instance, the mode conversion produced by a necessary right-angle bend in a differential interconnect can be effectively mitigated by using suitable rectangular length-match bumps.

The extent of mode conversion can be quantified by using full mixed-mode (MM) scattering (S) parameters [6]. In this paper, we consider two symmetric length match bumps to compensate a right-angle bend in a differential microstrip interconnect. We propose a formulation to optimize the full MM performance of this differential structure by efficiently using a subset of MM S-parameters. Our formulation combines global and local optimization methods (pattern search and Nelder-Mead), reducing the risk of falling into local minima, at a low computational cost. Our approach is validated by using several starting points. The MM performance before and after optimization is shown, confirming a substantial improvement.

II. Differential Microstrip Interconnect with a Right-Angle Bend and Length Match Bumps

The structure of interest is shown in Fig. 1. It consists of a differential microstrip interconnect pair with a 90° turn and two symmetric rectangular length match bumps. The microstrip

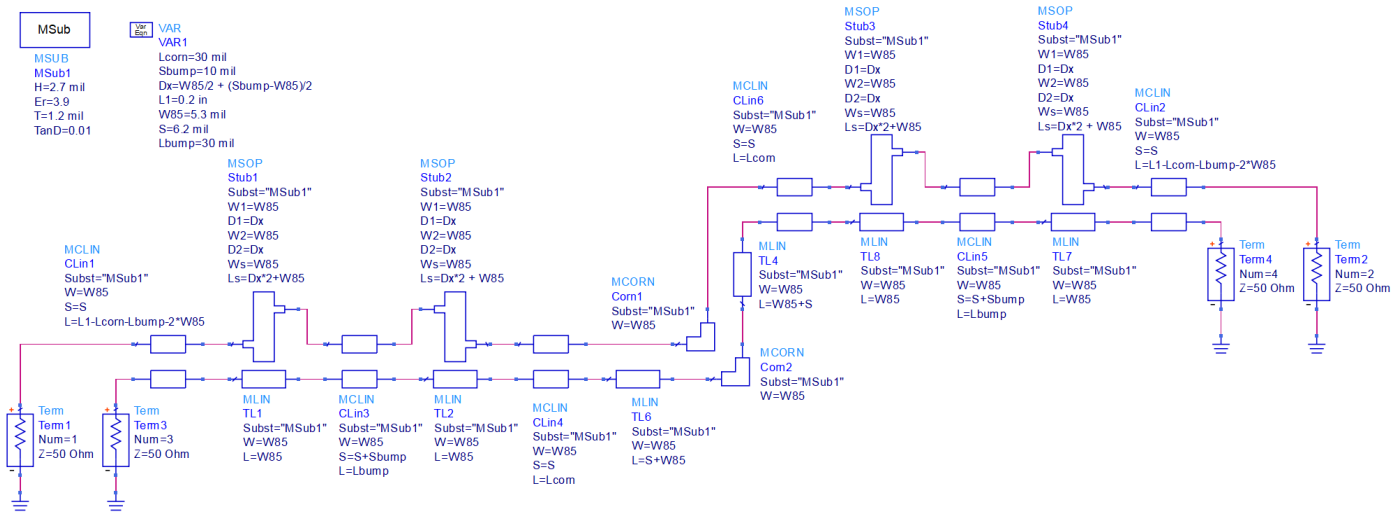

Fig. 2. ADS circuital model of the differential pair structure in Fig. 1.

$$\begin{bmatrix} S_{DD11} & S_{DD12} & S_{DC11} & S_{DC12} \\ S_{DD21} & S_{DD22} & S_{DC21} & S_{DC22} \\ S_{CD11} & S_{CD12} & S_{CC11} & S_{CC12} \\ S_{CD21} & S_{CD22} & S_{CC21} & S_{CC22} \end{bmatrix}$$

Fig. 3. The MM S-parameter matrix: S_{DD} refers to reliable data processing, S_{DC} refers to the conversion of noise into unreliable data (EMI susceptibility), S_{CD} refers to conversion of reliable data into noise (EMI emissions), and S_{CC} refers to processing of noise signals.

cross section is also shown in Fig. 1. The differential pair used has an 85-Ω differential impedance. It uses a substrate height H = 2.7 mils, a metal thickness t = 1.2 mils, a relative dielectric permittivity ε_r = 3.9, and a loss tangent $\tan(\delta)$ = 0.01. The trace width along the differential pair is W_{85} = 5.3 mils, the intra-pair spacing is S = 6.2 mils, and the differential main length is L_1 = 200 mils. The length match bump dimension is controlled by the variables L_{bump} and S_{bump}. The proximity of the bump to the 90° corner is controlled by the variable L_{corn}.

We confirm the differential impedance of the microstrip pair shown in Fig. 1 using ADS LineCalc [5]. The differential impedance of the coupled structure is $Z_{diff} = 2Z_{odd} = 2(42.509\ \Omega) = 85.018\ \Omega$, where Z_{odd} is the odd-mode impedance.

The interconnect structure is implemented in Keysight ADS as shown in Fig. 2. It uses microstrip coupled lines (MCLIN), SE microstrip lines (MLIN), symmetric pair of open stubs (MSOP), and 90° microstrip bends (MCORN). Components MSOP, MLIN, and MCLIN are used to implement the bumps.

We use MATLAB to drive ADS and perform parametric simulations and numerical optimization. The SE S-parameter results obtained from Keysight ADS, are converted using MATLAB into full MM S-parameters (see Fig. 3) following [6].

Given that the MM S-parameters matrix is symmetric for any reciprocal network [6], we need to consider only 10 out of the 16 MM S-parameters (see Fig. 3). Additionally, since the microstrip structure in Fig. 1 is not only reciprocal but also physically symmetric, then $S_{CD11} = S_{CD22}$, $S_{CD12} = S_{CD21}$, $S_{DD11} = S_{DD22}$, $S_{DD21} = S_{DD12}$, $S_{CC11} = S_{CC22}$, and $S_{CC12} = S_{CC21}$, which allows us to further reduce the set of MM S-parameters from 10 to only 6. The six relevant responses (S_{CD}, S_{DD}, and S_{CC}) for the interconnect with no bumps compensation are shown in Fig. 4, using a typical frequency band (0-20 GHz) suitable for modern high-speed differential interconnects, showing the negative effect caused by the right-angle bend.

III. Optimizing the Two Symmetric Length Match Bumps Considering the Full Mixed-Mode Performance

The proposed bump optimization follows a general formulation for nominal design optimization [7]. The circuit simulation responses are denoted by $\boldsymbol{R}$,

$$\boldsymbol{R} = \boldsymbol{R}(\boldsymbol{x}, \boldsymbol{z}, \boldsymbol{\psi}) \quad (1)$$

where $\boldsymbol{x}$ contains the optimization variables, $\boldsymbol{z}$ contains the pre-assigned parameters, and $\boldsymbol{\psi}$ contains the independent

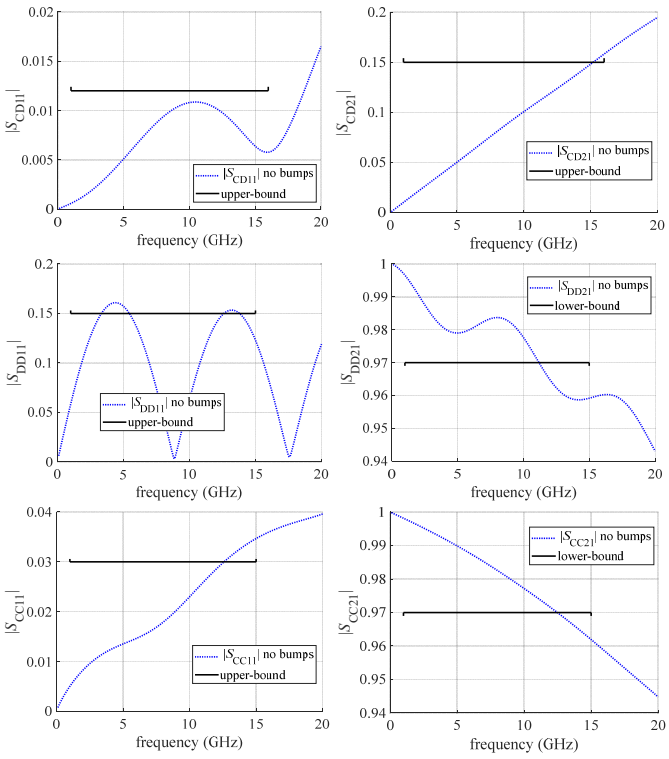

Fig. 4. The relevant MM S-parameters of the differential microstrip structure in Fig. 1 when no bumps are used (when S_{bump} = 0).

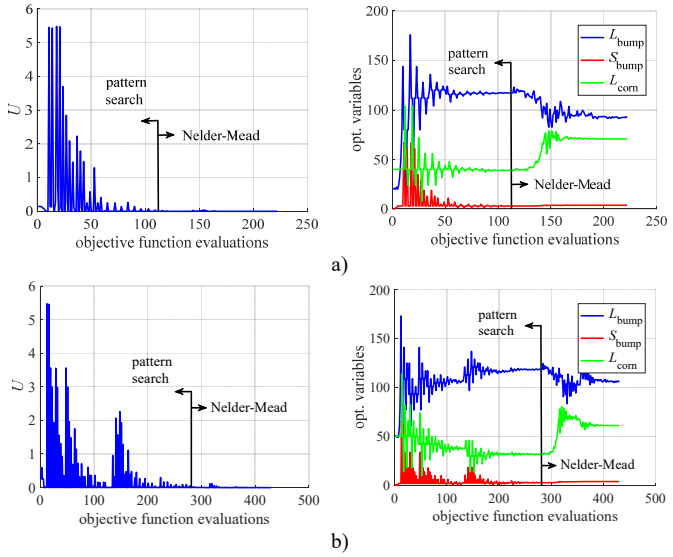

Fig. 5. Optimization results combining pattern search and Nelder-Mead: evolution of the objective function, and evolution of the optimization variables. a) when $\boldsymbol{x}^{(0)} = [20\ \ 0\ \ 40]^{\mathrm{T}}$, switching from pattern search to Nelder-Mead occurs at objective function evaluation number 114; b) when $\boldsymbol{x}^{(0)} = [50\ \ 0\ \ 50]^{\mathrm{T}}$, that switching occurs at evaluation 283.

simulation variables. The variables used to optimize the bump dimension are: $\boldsymbol{x} = [L_{\mathrm{bump}}\ \ S_{\mathrm{bump}}\ \ L_{\mathrm{corn}}]^{\mathrm{T}}$, the pre-assigned (fixed) parameters are: $\boldsymbol{z} = [H\ \ \varepsilon_{\mathrm{r}}\ \ \tan(\delta)\ \ t\ \ W_{85}\ \ S\ \ L_1]^{\mathrm{T}}$, and the independent variables for the simulator are: $\boldsymbol{\psi} = [units, IF, FF, FP]^{\mathrm{T}}$, where *units* is set in mils, *IF* is the initial simulated frequency, *FP* is the number of frequency points per frequency sweep, and *FF* is the final simulated frequency.

The design problem of this circuit can be formulated as [8],

$$\boldsymbol{x}^* = \arg\min_{\boldsymbol{x}} U\big(\boldsymbol{R}(\boldsymbol{x}, \boldsymbol{z}, \boldsymbol{\psi})\big) \tag{2}$$

where $\boldsymbol{x}^*$ is the optimal design of an unconstrained optimization problem and U is a suitable objective function defined in terms of the design specifications.

Our objective function U follows a minimax formulation with no constraints,

$$U(\boldsymbol{x}) = \max\{\ldots \boldsymbol{e}_k(\boldsymbol{x}) \ldots\} \tag{3}$$

where the $k^{\text{-th}}$ error vector function $\boldsymbol{e}_{\mathrm{k}}(\boldsymbol{x})$ is normalized with respect to each specification limit using only the relevant MM S-parameters mentioned in Section II, as follows:

$$\boldsymbol{e}_k(\boldsymbol{x}) = \begin{bmatrix} \dfrac{|S_{\mathrm{DD11}}|}{0.015} - 1 \\ \dfrac{|S_{\mathrm{CC11}}|}{0.030} - 1 \\ \dfrac{-|S_{\mathrm{DD21}}|}{0.97} + 1 \\ \dfrac{|S_{\mathrm{CD21}}|}{0.15} - 1 \\ \dfrac{-|S_{\mathrm{CC21}}|}{0.97} + 1 \\ \dfrac{|S_{\mathrm{CD11}}|}{0.012} - 1 \end{bmatrix} \tag{4}$$

The specification limits used in (4) over the frequency band illustrated in Fig. 4 were selected arbitrarily but considering a feasible performance for the interconnect. We solve (2) by using a combination of heuristic global and local optimization methods, namely, pattern search and Nelder-Mead. We start

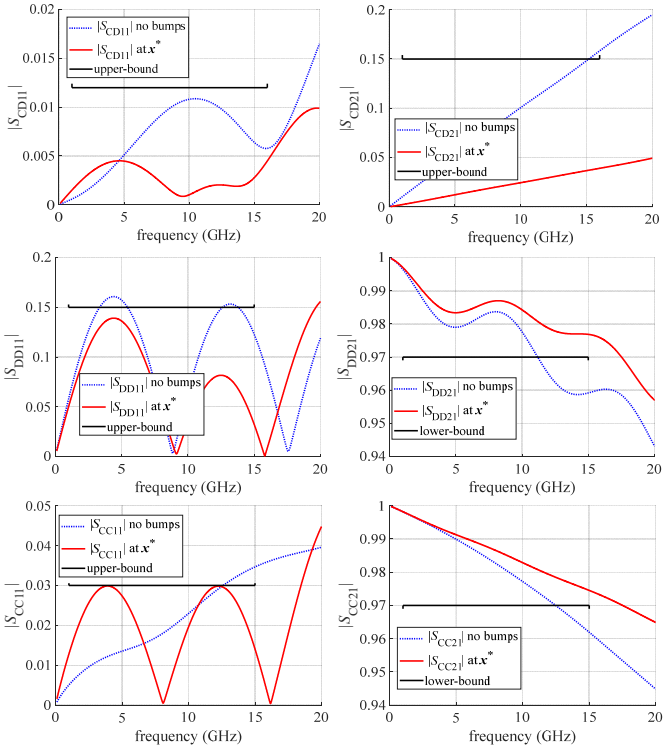

Fig. 6. The relevant MM S-parameters of the microstrip differential interconnect in Fig. 1 at the starting point (with no length match bumps) and after optimizing the length match bumps.

with pattern search to explore the design space, followed by an automated switch to Nelder-Mead (based on the termination criteria), as in [9]. In contrast to using classical global methods such as genetic algorithms, which require too many function evaluations, the proposed combination allows escaping from poor local minima at a low computational cost. The optimization runs on a conventional computer (Core i7 at 2.3 GHz, with 48 GB RAM and 500 GB solid state drive).

Several starting points are used to assess the capability to escape from poor local minima. The corresponding results are shown in Table I. All the starting points correspond to a structure with no bump compensation ($S_{\mathrm{bump}} = 0$). Only the first optimization seed resulted in a poor local minimum (positive objective function, indicating that the design specifications are violated). The remaining starting points yield consistent optimal designs that satisfy the design specifications. The second-best result in Table I is shown in Fig. 5a, with a seed $\boldsymbol{x}^{(0)} = [20\ \ 0\ \ 40]^{\mathrm{T}}$, yielding $U(\boldsymbol{x}^*) = -0.002746$, and $\boldsymbol{x}^* = [92.46\ \ 3.79\ \ 70.71]^{\mathrm{T}}$. Notice that the switching from pattern search to Nelder-Mead occurs at objective function evaluation (OFE) number 114. The best optimal design in Table I is shown in Fig.

TABLE I. OPTIMIZATION RESULTS FOR DIFFERENTIAL INTERCONNECT WITH RIGHT ANGLE BEND AND TWO SYMMETRICAL BUMPS

$\boldsymbol{x}^{(0)}$ (mils)	$U(\boldsymbol{x}^*)$	$\boldsymbol{x}^*$ (mils)	iter	OFE	opt. time (minutes)
$[10\ \ 0\ \ 20]^{\mathrm{T}}$	+0.121860	$[46.75\ \ 0\ \ 20]^{\mathrm{T}}$	63	75	3.45
$[20\ \ 0\ \ 40]^{\mathrm{T}}$	–0.002746	$[92.46\ \ 3.79\ \ 70.71]^{\mathrm{T}}$	85	222	3.18
$[40\ \ 0\ \ 40]^{\mathrm{T}}$	–0.002746	$[92.46\ \ 3.79\ \ 70.71]^{\mathrm{T}}$	87	235	3.26
$[10\ \ 0\ \ 10]^{\mathrm{T}}$	–0.002948	$[106.30\ \ 3.98\ \ 61.18]^{\mathrm{T}}$	154	460	5.73
$[50\ \ 0\ \ 50]^{\mathrm{T}}$	–0.002948	$[106.30\ \ 3.98\ \ 61.18]^{\mathrm{T}}$	146	430	5.38
$[60\ \ 0\ \ 60]^{\mathrm{T}}$	–0.002948	$[106.30\ \ 3.98\ \ 61.18]^{\mathrm{T}}$	160	496	6.19

5b, with a seed $\boldsymbol{x}^{(0)} = [50 \;\; 0 \;\; 50]^{\mathrm{T}}$, yielding $U(\boldsymbol{x}^{*}) = -0.002948$, and $\boldsymbol{x}^{*} = [106.30 \;\; 3.98 \;\; 61.18]^{\mathrm{T}}$. In this case, switching from pattern search to Nelder-Mead occurs at OFE number 283.

The MM S-parameters of interest before and after optimization are shown in Fig. 6. These responses correspond to the results obtained with seed $\boldsymbol{x}^{(0)} = [50 \;\; 0 \;\; 50]^{\mathrm{T}}$, at which the structure initially violates the great majority of the design specifications. The results confirm that the performance of the optimized structure is significantly better than that one with no length-match bumps. All the relevant MM S-parameters of the optimized structure satisfy the design specifications.

IV. Conclusion

The mode conversion caused by a necessary right-angle bend in a microstrip differential interconnect was effectively mitigated in this paper by optimizing two rectangular length-match bumps. Our proposed formulation efficiently optimizes the full mixed-mode S-parameters performance. It combines heuristic global and local optimization methods to reduce, with a low computation cost, the likeliness of falling into local minima. Consistent results in performance improvement of the relevant MM S-parameters after the optimization process using several starting points validate our approach. In future work, full-wave EM simulations of this same structure will be addressed.

References

[1] S. Connor, B. Archambeault, and M. Mondal, "The impact of common mode currents on signal integrity and EMI in high-speed differential data links", in *IEEE Int. Symp. Electromagn. Compat.*, Detroit, MI, USA, Aug. 2008, pp. 1-5.

[2] A. Jaze, B. Archambeault, and S. Connor, "Differential mode to common mode conversion on differential signal vias due to asymmetric GND via configurations," in *IEEE Int. Symp. Electromagn. Compat.*, Denver, CO, USA, Aug. 2013, pp 735-740.

[3] H. Zhang, S. Krooswyk, and J. Ou, *High Speed Digital Design, Design of High Speed Interconnects and Signaling*. Walthman, MA, USA: Elsevier, 2015.

[4] M. R. Burford, P. A. Levin, and T. J. Kazmierski "Skew and EMI management in differential microstrip lines up to 15GHz," in *IEEE Workshop on Signal Prop. on Interconnects*, Ruta di Camogli, Itali, 2007, pp 188-191.

[5] LineCalc, Agilent Technologies., Palo Alto, CA, USA, 2004.

[6] S. H. Hall and H. Heck, *Advanced Signal Integrity for High-Speed Digital Designs*. Hoboken, NJ: Wiley-IEEE, 2009.

[7] X. Yang, *Engineering Optimization an Introduction with Metaheuristic Applications*. Hoboken, NJ: John Wiley & Sons, Inc., 2010.

[8] J. W. Bandler and J. E. Rayas-Sánchez, "An early history of optimization technology for automated design of microwave circuits," *IEEE J. of Microw.*, vol. 3, no. 1, pp. 319-337, Jan. 2023.

[9] F. E. Rangel-Patiño, J. E. Rayas-Sánchez, E. A. Vega-Ochoa, and N. Hakim, "Direct optimization of a PCI Express link equalization in industrial post-silicon validation," in *IEEE Latin American Test Symp. (LATS 2018)*, Sao Paulo, Brazil, Mar. 2018, pp. 1-6.